Cost-Effectiveness Hybrid Permanent Magnet Assisted Synchronous Reluctance Machine for Electric Vehicle

Hoyun Won
Department of Electrical and
Computer Engineering
The University of Alabama
Tuscaloosa, AL, USA
hwon@crimson.ua.edu

Yang-Ki Hong Department of Electrical and Computer Engineering The University of Alabama Tuscaloosa, AL, USA ykhong@eng.ua.edu

Minyeong Choi Department of Electrical and Computer Engineering The University of Alabama Tuscaloosa, AL, USA mchoil 1@crimson.ua.edu Briana Bryant
Department of Electrical and
Computer Engineering
The University of Alabama
Tuscaloosa, AL, USA
bmbryant1@crimson.ua.edu

Jonathan Platt
Department of Electrical and
Computer Engineering
The University of Alabama
Tuscaloosa, AL, USA
jtplatt@crimson.ua.edu

Seungdeog Choi Department of Electrical and Computer Engineering Mississippi State University Starkville, MS, USA seungdeog@ece.msstate.edu

Abstract— This paper investigates a three-layer hybrid permanent magnet assisted synchronous reluctance machine (H-PMASynRM) that exhibits the most cost-effective performance for electric vehicle applications. Two kinds of permanent magnet, ferrite and NdFeB, are interchangeably used to evaluate motor performance metrics such as the torque per cost, torque density, efficiency, peak power factor, maximum speed, and rate of irreversible demagnetization. The simulation results show that the H-PMASynRM having the first layer made of NdFeB, the second layer made of ferrite, and the third layer made of a combination of ferrite and NdFeB, can exhibit the same maximum torque of 220 Nm with \$12 lower cost, 1-3% higher efficiency at speed above 8,000 rpm, 6.8% lower peak power factor, and only 17% lower torque density compared to the NdFeB-based V-type PMSM that is used in Toyota Prius 2010.

Keywords— Hybrid permanent magnet synchronous reluctance motor, ferrite, electric vehicle

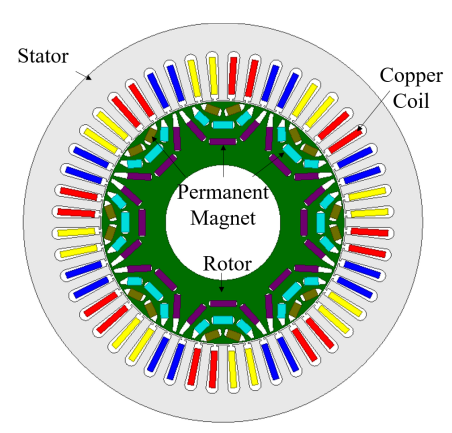
I. INTRODUCTION

Due to their high torque density, maximum speed, and efficiency, rare-earth-based permanent magnet synchronous motors (PMSM) are widely used in commercial vehicles [1,2]. However, the volatile supply and price of rare-earth materials makes it difficult for automakers to produce these motors consistently with a low cost [1]. Owing to these significant drawbacks, a low-cost ferrite-based PMSM with a stable supply chain has received much attention [1-2]. Among various ferrite-based PMSMs, a permanent magnet assisted synchronous reluctance motor (PMASynRM) showed the most promising performance by compensating for a low PM torque from the low magnetic properties of the ferrite with a high reluctance torque from a high saliency ratio [2]. Out of the reported ferrite-based

PMASynRM, a three-layer PMASynRM with rectangular-shaped ferrite magnets, as illustrated in Fig. 1, exhibits high torque and maximum speed with easy manufacturability and low cost [2]. Despite its cost advantages over the rare-earth based PMSM, the proposed design still suffers from 25.5 % lower torque density compared to the rare-earth based PMSM and high rate of the irreversible demagnetization of the ferrite magnet.

Thus, to increase the torque density and reduce the rate of the irreversible demagnetization, a hybrid ferrite/NdFeB-based PMASynRM (H-PMASynRM) has aroused considerable attention [3,4]. W. Yu investigated saliency and use of PM in the H-PMASynRM to reduce the usage of rare-earth materials [3]. However, the paper only investigated the designs with middle, arc-shaped, and sandwiched ferrite/NdFeB PMs and did not address the cost-related performance. Although M. Hofer investigated the two-layer H-PMASynRM, only two cases were considered: 1) ferrites in both layer and 2) ferrites in top layer and NdFeB in bottom layer [4]. Accordingly, there is a lack of studies that report on the H-PMASynRM with various ferrite/NdFeB combinations for achieving cost effective performance.

Thus, this paper investigates 32 different ferrite/NdFeB combinations in the three-layer H-PMASynRM with rectangular-shaped PMs to produce the most cost-effective performance. To determine the most cost-effective performance, the torque per cost, torque ripple, efficiency, power factor, base and maximum speed, and demagnetization of various combinations of H-PMASynRM are simulated and compared with those of the baseline motor, which is the rare-earth based motor used in the Toyota Prius, referred to in this paper as the Prius motor. ANSYS Maxwell 2D and 3D-finite element



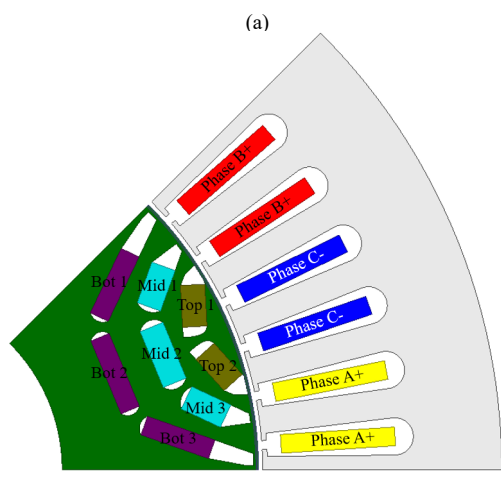


Fig. 1. Design of hybrid permanent magnet assisted synchronous reluctance machine (H-PMASynRM): (a) Overall view and (b) 1/8th view.

TABLE I. SPECIFICATIONS OF H-PMASYNRM AND PRIUS MOTOR [6].

Parameter	Value
Stator Outer/inner diameter [mm]	264/161.9
Rotor Outer/inner diameter [mm]	160.4/76
Stack Length [mm]	50.8
Number of slot/pole	48/8
Number of turns	11
Maximum current [A _{rms}]	177
Soft Iron Core Material	M19-29G

analysis (FEA) v.18.1 is used to simulate the motor performance, while ANSYS Mechanical is used to analyze the mechanical stress on the rotor.

II. DESIGN SPECIFICATION AND SIMULATION SETUP

Fig. 1 shows the configuration and details of the three-layer H-PMASynRM, while Table I shows the specifications. To quantitatively assess the effectiveness of the three-layer H-PMASynRM, the same PMSM design specifications of the Prius motor are used [6]. For the ferrite PM, Hitachi NMF-12F, which has a remanent flux density of 0.46 T and coercivity of 329 kA/m in room temperature, is used [7], while for the NdFeB PM, Hitachi NMX-37F, which has a remanent flux density of 1.23 T

TABLE II. MATERIAL COST [5].

Material	Cost (\$/kg)	Density (g/cm³)
NdFeB	100	7.5
Ferrite	7	5
Copper	7.03	8.96
M19-29G	1.0	7.85

and coercivity of 942 kA/m in room temperature, is utilized [8]. These two types of PMs are used and combined accordingly for the PM denoted in Fig. 1 (b). In this paper, the PMs closest to the outer rotor are designated as "Top 1 and 2", while the PMs on the next closest and farthest from the outer rotor are called "Mid 1, 2, and 3" and "Bot 1, 2, and 3", respectively. Since the motor is required to rotate both ways, symmetrical PM combinations, e.g., the same ferrite or NdFeB PM for Top 1 and 2, Mid 1 and 3, and Bot 1 and 3, are considered.

In total, there are 32 different combinations of ferrite and NdFeB PMs to assess for motor performance, where these combinations can be divided into 4 sets as follows

- Set 1: Top, middle, and bottom PMs are either all ferrite or NdFeB.
- Set 2: Top and bottom PMs are either all ferrite or NdFeB, while middle PMs are a combination of either ferrite/NdFeB/ferrite or NdFeB/ferrite/NdFeB.
- Set 3: Top and middle PMs are either all ferrite or NdFeB, while bottom PMs are a combination of either ferrite/NdFeB/ferrite or NdFeB/ferrite/NdFeB.
- Set 4: Top PMs are either all ferrite or NdFeB, while middle and bottom PMs are a combination of either ferrite/NdFeB/ferrite or NdFeB/ferrite/NdFeB.

III. RESULT AND DISCUSSION

Since the main objective of this paper is to evaluate the motor performance versus motor cost, the cost of the motor is first calculated as follows

$$\begin{aligned} Machine \, Cost &= (A_{Nd} \, \rho_{Nd} \, C_{Nd} + A_{fe} \, \rho_{fe} \, C_{fe} + A_{ro} \, \rho_{M19} \, C_{M19} \\ &+ A_{st} \, \rho_{M19} \, C_{M19}) L + 3N A_{cu} \big(2 \big(L + 2 L_{end} \big) \rho_{cu} \big) C_{cu} \end{aligned} \tag{1}$$

where A denotes the area for each material, ρ is the density, C is the material cost per kg, the subscripts correspond to Nd = NdFeB, fe = ferrite, M19 = M19-29G, and cu = copper, L is the stack length of the motor, N is the number of turns, and L_{end} is the end-winding length of one side. The cost of each material is summarized in Table II [5]. The price of NdFeB PM is estimated as \$100/kg based on U.S. Geological Survey Data, which reported that the price of neodymium oxide and dysprosium as \$51/kg and \$180/kg, respectively [5]. To ease the calculation, the cost of lamination between stacked cores is excluded.

A. Optimal PM Combination Selection Based on Performance

First, the torque and torque/dollar of the targeted Prius motor under the 250 A peak current are simulated using ANSYS 2D-FEA and compared with those of the H-PMASynRM with 32

TABLE III. PM LISTS OF H-PMASYNRM EHXIBITHING HIGHER TOROUE/COST THAN PRIUS MOTOR AND TOROUE RIPPLE BELOW 38 %.

No.	W4	M2	В3	В7	В8
Top 1	Nd	Nd	Nd	Fe	Fe
Top 2	Nd	Nd	Nd	Fe	Fe
Mid 1	Fe	Fe	Fe	Fe	Fe
Mid 2	Fe	Nd	Fe	Fe	Fe
Mid 3	Fe	Fe	Fe	Fe	Fe
Bot 1	Fe	Fe	Fe	Fe	Fe
Bot 2	Fe	Fe	Nd	Nd	Fe
Bot 3	Fe	Fe	Fe	Fe	Nd

different PM combinations under the same motor specifications shown in Table I. The simulation shows that the Prius motor exhibits a torque of 220 Nm and a torque/dollar of 2.69 Nm/\$. Among 32 different PM combinations, there are only 5 combinations in the H-PMASynRM that show a higher torque/dollar than the Prius motor and a torque ripple below 38 %. Table III shows the list of the H-PMASynRM with PM combinations that exhibit higher torque/dollar than the Prius motor, while Table IV summarizes the motor performance of the listed H-PMASynRMs. The results show that the H-PMASynRM can save \$23-\$51 and produce 0.48 to 2.43 higher torque per dollar than the Prius motor.

Then, to further evaluate the motor performance quantitatively, the stack lengths of the H-PMASynRMs with these combinations are increased accordingly so that the same maximum torque of 220 Nm can be produced for the H-PMASynRMs and the Prius motor. Table V shows the simulated maximum torque, stack length, total cost, torque/dollar, torque density, peak power factor, rate of irreversible demagnetization at the peak current of 250 A, base and maximum speed, and torque at 10,000 rpm, while Fig. 2 shows the efficiency map of the H-PMASynRM with these 5 combinations and the Prius motor. To calculate the base and maximum speed, torque at 10,000 rpm, and efficiency map, the Electric Machine Design Toolkits in ANSYS Maxwell are used. Maximum torque per ampere (MTPA) control is utilized below the base speed. Above the base speed, flux weakening control is employed to adjust the d- and q-axis current to keep the induced back-EMF below the maximum controllable voltage (Vcont) and input current below maximum allowable current, which is 177 A_{rms} for Prius motor. When both the induced back-EMF and input current reach their maximum, the motor reaches its maximum speed. The V_{cont} is calculated by the type of the switching control scheme and maximum battery voltage (V_{bat}). Since the paper uses a space vector-pulse width modulation (SVPWM) to control the switches and V_{bat} of 500V, the V_{cont} is calculated as 389 V.

The rate of the irreversible demagnetization (α) of the PM is calculated by

$$\alpha = A_{irrev \ demag} / A_{tot \ mag}, \qquad (1)$$

where A_{irrev_demag} is the area where the flux density is below a threshold value and the A_{tot_mag} is the total PM area. This threshold flux density value (B_{thr}) is when the magnetization (M)

TABLE IV. MOTOR PERFORMANCE OF H-PMASYNRM EHXIBITHING HIGHER TORQUE/COST THAN PRIUS MOTOR AND TORQUE RIPPLE BELOW 38 %

No.	Torque (Nm)	Torque ripple (%)	Cost (\$)	Torque/ Cost (Nm/\$)
W4	170.4	35.4	38.8	4.39
M2	182.7	37.8	58.5	3.12
В3	186.8	36.8	59.4	3.14
B7	164.3	35.7	32.3	5.07
B8	171.8	34.8	49.0	3.50

of the material reaches its knee point, or $M=0.9M_{sat}$, in its 2^{nd} quadrant on the M-H characteristics, where M_{sat} is the saturation magnetization [9]. When the M is below the knee point, the loss is non-recoverable. This means that the flux density of the magnet does not go to its remanent flux density if the applied field is reduced to zero, but to reduced flux density. Table VI shows the threshold flux density value of the ferrite PM when its $M=0.9~M_{sat}$ for different temperature. Only the value of the ferrite PMs is given because the operating flux density of the NdFeB magnet are higher than its threshold value in all operating temperature.

The efficiency (η) at desired torque (T_{tot}) and speed (ω_m) is computed by using following equation

$$\eta = \frac{P_{out}}{P_{in}} = \frac{T_{tot}\omega_m}{T_{tot}\omega_m + Losses},$$
(2)

where P_{in} and P_{out} are the input and output power, whereas *Losses* comprises of the solid, winding, and core loss.

The simulation results show that even if the stack length of the H-PMASynRM is increased, the H-PMASynRM can save \$12-40 and produce 0.47-2.44 higher torque per dollar than the Prius motor. Furthermore, as Fig. 2 clearly illustrates, the H-PMASynRM exhibits 1-3% higher efficiency than the Prius motor when the motor speed exceeds 8,000 rpm. In addition, a higher efficiency at speeds above 8000 rpm and a larger peak efficiency region are observed for the H-PMASynRM in combinations that have NdFeB in the third layer. As illustrated in Fig. 3, this is mainly attributed to the lower flux density between the second and third layer for the H-PMASynRM having NdFeB in the third layer, resulting in lower core loss. However, it is noted that the proposed H-PMASynRM exhibits 6.8-24.7 % lower peak power factor compared to that of the Prius motor.

Among these combinations, the B3 combination exhibits the most promising performance with its shortest stack length of 60.5 mm, highest torque density of 66.2 Nm/L, good torque/cost of 3.11 Nm/\$, high peak power factor of 0.85, good demagnetization rate of 1 % under 250 A peak current, highest maximum speed of 12,000 rpm, and highest torque of 51.7 Nm at 10,000 rpm. Compared to the Prius motor, the H-PMASynRM with the B3 combination achieves the same maximum torque of 220 Nm with an only 10 mm longer stack length, \$12.6 lower cost, 0.47 Nm/\$ higher torque per cost, 6.8 % lower peak power factor, 17.5 % lower torque density, and 9.9 % lower maximum

TABLE V. MOTOR PERFORMANCE COMPARISON BETWEEN PRIUS MOTOR AND H-PMASYNRM EXHIBITING HIGHER TORQUE/COST THAN PRIUS MOTOR .

Motor	Maximum Torque (Nm)	Torque ripple (%)	Stack Length (mm)	Total Cost (\$)	Torque/ Cost (Nm/\$)	Torque Density (Nm/L)	Peak power factor	Demagnetization Rate at 250A (%)	Base/ Maximum Speed (rpm)	Torque at 10,000 rpm (Nm)
W4	220	35.4	66	52.0	4.36	60.9	0.77	0	2850/10250	35.8
M2	220	37.8	61	70.3	3.11	65.9	0.75	2	3100/10300	42.5
В3	220	36.8	60.5	70.7	3.12	66.4	0.85	0	3000/12000	51.7
B7	220	35.7	68	43.3	5.06	59.1	0.71	28	2350/11500	38.0
B8	220	34.8	65.5	63.2	3.48	61.3	0.73	15	2800/11500	39.6
Prius Motor	220	24.0	50.8	83.3	2.64	79.1	0.91	0	3000/13250	62.1

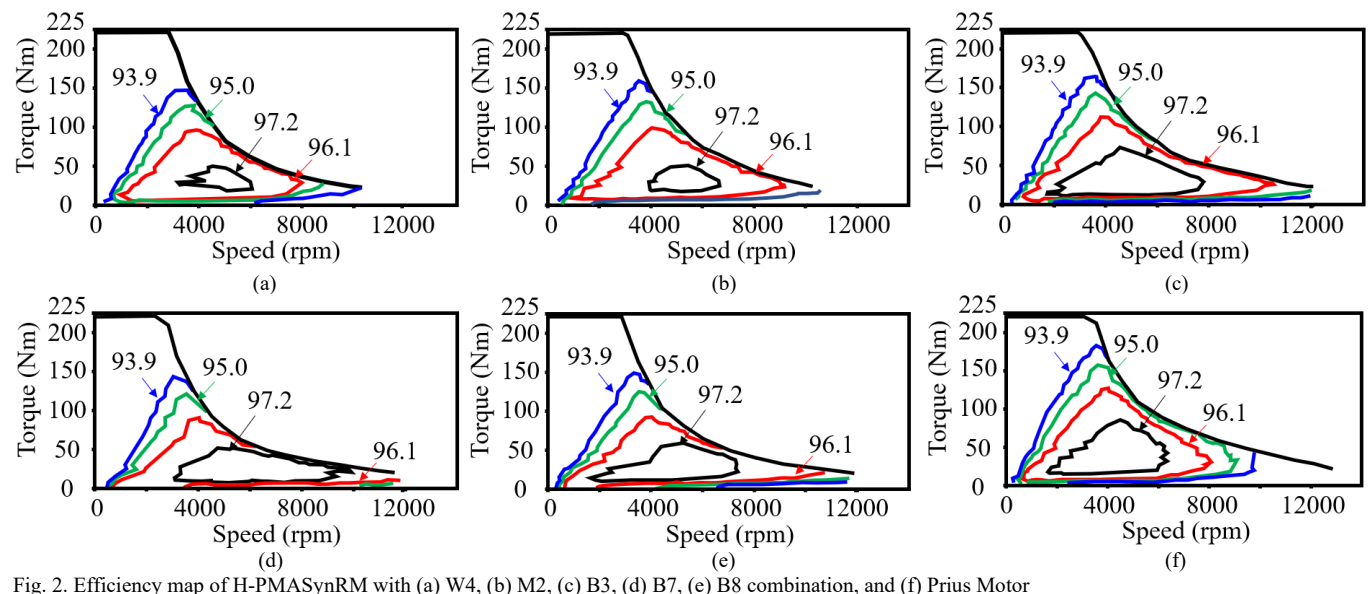


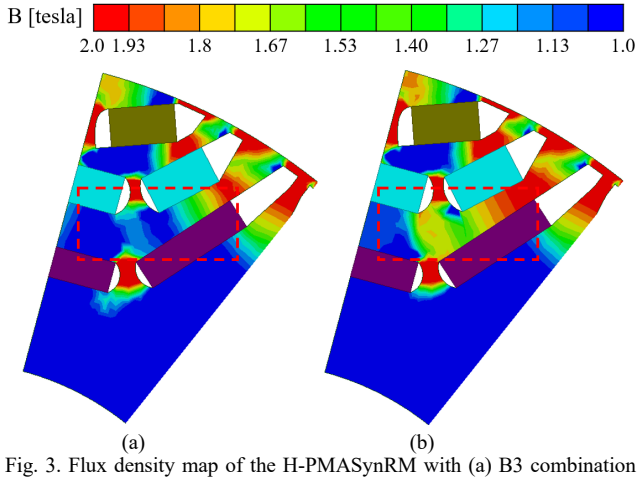
TABLE VI. THRESHOLD FLUX DENSITY FOR DIFFERENT OPERATING FERRITE TEMPERATURE

Temperature (°C)	Threshold Flux Density of Ferrite (T)
-40	0.1
20	0
60	-0.07
100	-0.1

speed. Thus, the H-PMASynRM with the B3 combination is selected to further investigate its performance.

B. Effects of Temperature on the Performance

The effects of the temperature ranging from -40 to 100 °C on the torque, torque ripple and α performance are evaluated. Generally, the motor sustains its operation under a hot temperature due to the winding and core losses and a cold temperature in cold driving area. Fig. 4 shows the torque and torque ripple performance. As expected, the torque decreases as the temperature increases, due to the negative temperature coefficient of remanence. On the other hand, the torque ripple



and (b) W4 combination.

is unaffected by the temperature change. From the simulation, it is noted that only the flux density of the Bot 3 PM shows lower than the B_{thr} listed in Table VI. Thus, only Bot 3 is selected to analyze the a. Fig. 5 shows the flux density distribution of Bot 3 PM with various temperatures at the maximum peak current of 250 A. By using the B_{thr} listed in Table VI, the α are calculated

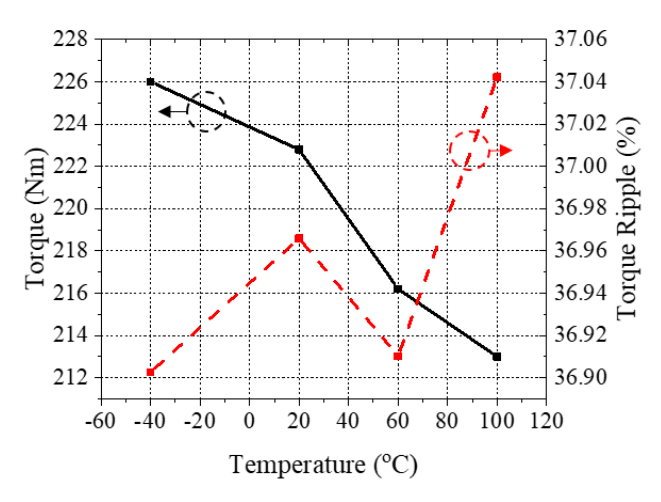


Fig. 4. Torque and torque ripple performance of the H-PMASynRM with B3 combination for various magnet temperature.

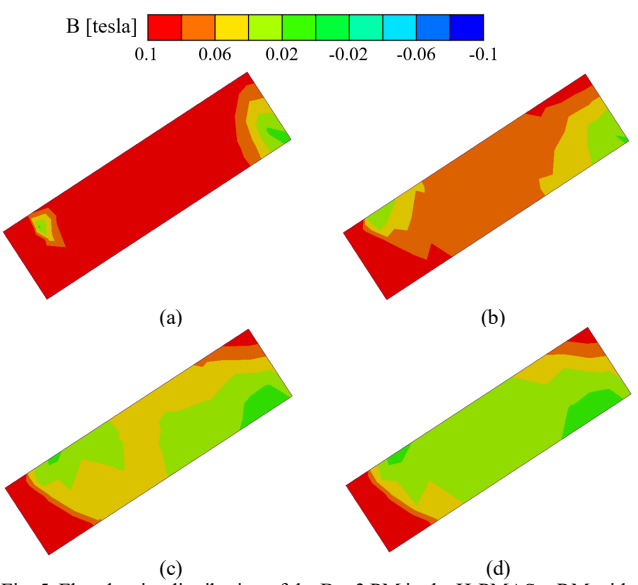


Fig. 5. Flux density distribution of the Bot 3 PM in the H-PMASynRM with B3 combination for (a) -40, (b) 20, (c) 60, and (d) 100 °C.

as 10, 0, 0, and 0 % for the temperature of -40, 20, 60, and 100 °C. Other than the temperature at -40 °C, the motor operates without experiencing irreversible demagnetization.

C. Mechanical Stress Analysis

ANSYS Mechanical FEA tool is used to evaluate the mechanical strength of the motor. Fig. 6 shows the stress distribution of the proposed H-PMASynRM with the B3 combination at the maximum speed of 12,000 rpm. The results show that high von Mises stress is observed on the bridge and ribs between the PMs in the top layer. However, the overall stress is well below the material's stress limit of 345 MPa. Thus, it is confirmed that the proposed rotor is safe to operate at its maximum speed of 12,000 rpm.

D. 3D-FEA Result

Lastly, the Prius and proposed motor are evaluated using ANSYS Maxwell 3D-FEA software to emulate the motor performance in real environment. Fig. 7 shows the peak torque

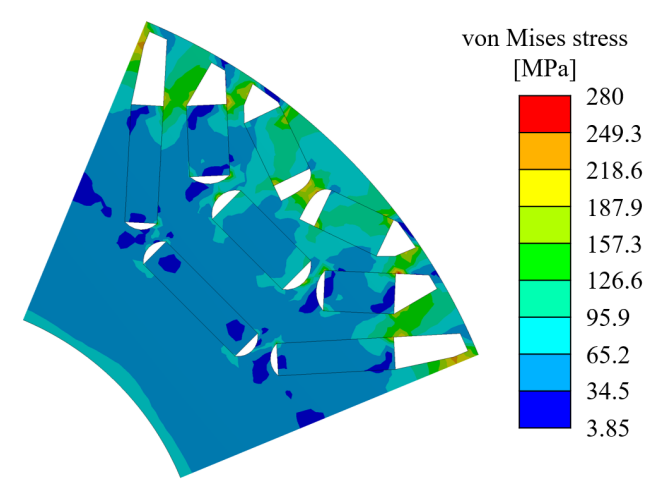


Fig. 6. Von Mises stresses distribution of the H-PMASynRM with B3 combination

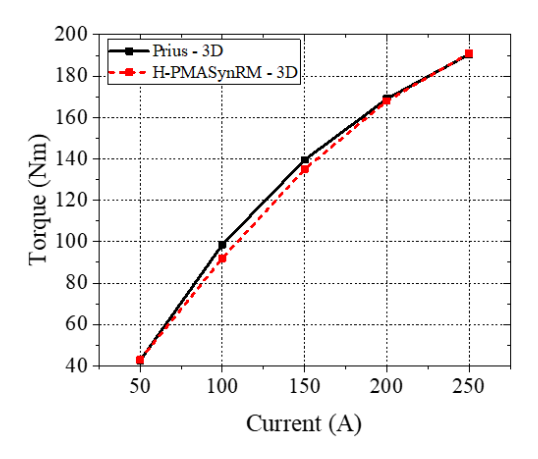


Fig. 7. 2D and 3D peak torque performance of the Prius motor and the proposed H-PMASynRM with B3 combination with various current.

performance of the Prius motor and proposed motor with B3 combination as a function of the peak phase current from 50 to 250 A. As shown clearly, the proposed motor exhibits a maximum torque of 190 Nm and shows similar torque performance compared to that of the Prius motor. This implies that the motor can be utilized in electric vehicle.

IV. CONCLUSION

This paper presented the most cost-effective permanent magnet (PM) combination comprised of rare-earth NdFeB and rare-earth-free ferrite PMs for the three-layer permanent magnet assisted synchronous reluctance machine (PMASynRM). To determine the most cost-effective PM combinations for the PMASynRM, we assessed the maximum torque, stack length, total cost, torque/dollar, torque density, peak power factor, demagnetization rate at the peak current of 250 A, base and maximum speed, and torque at 10,000 rpm for 32 different PM combinations in the PMASynRM and compared them with the motor used in Toyota Prius hybrid electric vehicle. The simulation results showed that the PMASynRM having the first layer made of NdFeB PM, the second layer made of ferrite PM, and the third layer made of a combination of ferrite and NdFeB, showed the same maximum torque of 220 Nm with a \$12.6

lower cost, 0.47 Nm/\$ higher torque per cost, only 10 mm longer stack length, 17.5 % lower torque density, 6.8% lower power factor, and 9.9 % lower maximum speed. Further, the mechanical stress analysis showed that the rotor can operate at its maximum speed of 12,000 rpm safely.

REFERENCES

- H. Won, Y. K. Hong, W. Lee, M. Choi, S. Li, and H. Yoon, "Low Torque Ripple Spoke-type Permanent Magnet Motor for Electric Vehicle," 2019 IEEE Interntional Electric Machine & Drives Conference, pp. 1-6, May 2019.
- [2] B M. Obata, S. Morimoto, M. Sanada, and Y. Inoue, "Performance of PMASynRM With Ferrite Magnets for EV/HEV Applications Considering Productivity," IEEE Trans. Ind. Appl., vol. 50, no. 4, pp. 2427-2435, Jul/Aug. 2014.
- [3] W. Wu, X. Zhu, L. Quan, Y. Du, Z. Xiang, and X. Zhu, "Design and Analysis of a Hybrid Permanent Magnet Assisted Synchronous Reluctance Motor Considering Magnetic Saliency and PM Usage," IEEE Trans. Appl. Supercond., vol. 28, no. 3, pp. 5200306, Ap. 2018.

- [4] M. Hofer and M. Schrodl, "Investigation of Permanent Magnet Assisted Synchronous Reluctance Machines for Traction Drives in High Power Flux Weakening Operation," 2020 IEEE Transportation Electrification Conference & Expo, pp. 1-5, Jun. 2020.
- [5] Q. Ma, A. El-Refaie, and B. Lequesne, "Low-Cost Interior Permanent Magnet Machine With Multiple Magnet Types," IEEE Trans. Ind. Appl., vol. 56, no. 2, pp. 1452-1463, Mar/Apr. 2020.
- [6] M. Olszewski, "Evaluation of the 2010 Toyota Prius Hybrid Synergy Drive System," FY2011 Oak Ride National Laboratory Report, Mar. 2011.
- [7] Hitach-metals, "Ferrite Magnets," Hitachi-metals, LTD. Online, Available: http://www.hitachi-metals.co.jp/e/products/auto/el/p03_05.html.
- [8] Hitachi-metals, "Neodymium-Iron-Boron Magnets NEOMAX Series," Hitachi-metals, LTD. Online, Available: http://www.hitachi-metals.co.jp/e/products/auto/el/pdf/nmx_a.pdf.
- [9] J. Niedra, "M-H Characteristics and Demagentization Resistance of Samrium-Cobalt Permanent Magnets to 300 C," NASA Contractor Report 189194, Aug. 1992.